

NATIONAL TRANSPORTATION SAFETY BOARD

Office of Research and Engineering
Materials Laboratory Division
Washington, D.C. 20594



September 30, 2019

MATERIALS LABORATORY FACTUAL REPORT

Report No. 18-078

A. ACCIDENT INFORMATION

Place : Scottsdale, AZ
Date : April 9, 2018
Vehicle : Piper PA-24-260 (N9456P)
NTSB No. : WPR18FA119
Investigator : Maja Smith, AS-WPR

B. COMPONENTS EXAMINED

1. Number 3 cylinder intake outer-valve spring pieces (4 pieces) from a Lycoming IO-540-N1A5 (S/N L-8118-48) engine.

C. DOCUMENTS REVIEWED

1. N9456P Lycoming Single Engine Field Notes 05/25/2018. The following parts were also submitted to the laboratory, but not examined: number 3 cylinder and head assembly with associated valves, rod, inside intake rocker arm, valve guides, spring plates. The Lycoming Single Engine Field Notes adequately documented the conditions of the components listed above.

D. DETAILS OF THE EXAMINATION

The as-received fractured spring pieces are shown in Figure 1, approximately arranged in their positions preceding the fractures. Each fracture is numbered, and each face of each fracture is identified with the letters A and B as shown in the figure.

The submitted spring is a helical compression spring with the last coils closed and ground flat. The spring was fabricated from 0.1760 inch diameter steel wire. The inside spring diameter is 1.300 inch, the outside spring diameter is 1.650 inch, and the spring length could not be determined as it was fractured in four pieces.

Scanning electron microscope (SEM) images of each spring fracture surface are shown in Figures 2-12. Fracture surface observations are summarized in Table 1.

Table 1**Summary of Fracture Surface Observations**

Fracture location (Figure 1)	Fracture face (Figure 1)	Observation	Figure number
Fracture 1	A	Fracture face was obscured by mechanical contact damage, unable to determine fracture macro- and micro-mode.	Figure 2
	B	Fracture macro-mode is consistent with fatigue fracture (origin at a surface pit on the helix inside diameter) through 40% of the diameter, with final fracture due to micro-void coalescence overstress fracture. The surface pit is approximately 247 μm (0.009 inch) deep. Mechanical contact damage prohibited fracture micro-mode confirmation.	Figures 3, 4
Fracture 2	A	Fracture macro-mode revealed a flat fracture with crack progression lines, fracture micro-mode revealed fine striations indicating fatigue fracture (origin at a surface pit on the helix inside diameter) through 50% of the diameter, with final fracture due to micro-void coalescence overstress fracture. The surface pit is approximately 275 μm (0.010 inch) deep.	Figures 5, 6, 7, 8, 9
	B	Fracture macro-mode is consistent with fatigue fracture (origin obscured by mechanical contact damage).	Figures 10, 11
Fracture 3	A	Fracture face was nearly perpendicular to the wire axis and was obscured by mechanical damage, unable to determine the fracture origin or the fracture macro- and micro-mode.	Figure 12
	B	Fracture face was nearly perpendicular to the wire axis and was obscured by mechanical damage, unable to determine the fracture origin or the fracture macro- and micro-mode.	Figure 12

Fractures 1 and 2 initiated at pits on the inside diameter of the helix and propagated due to fatigue crack growth through about 40% to 50% of the diameter before final fracture due to overstress. The fractures propagated along a 45° plane that is consistent with the superposed direct-shear, torsional-shear, and curvature-shear stresses found in axially-loaded helical springs. Fracture 3 was nearly perpendicular to the wire axis and the fracture surfaces were obscured by mechanical damage; determination of the fracture origin or the fracture macro- and micro-mode was not possible.

Michael Budinski
Chief, Materials Laboratory Division

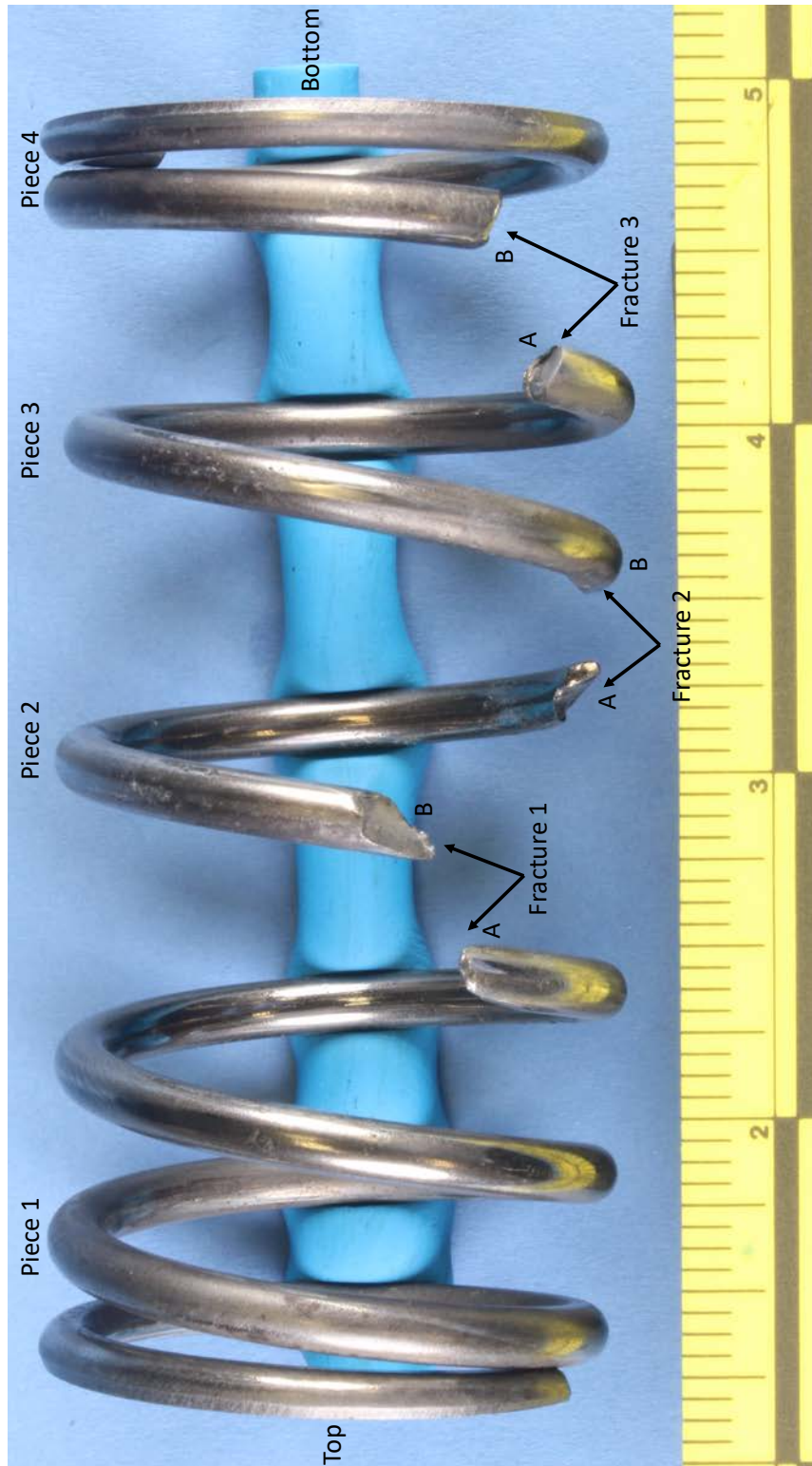


Figure 1 The as-received fractured spring pieces. The as-installed spring orientation (top and bottom) is also indicated.

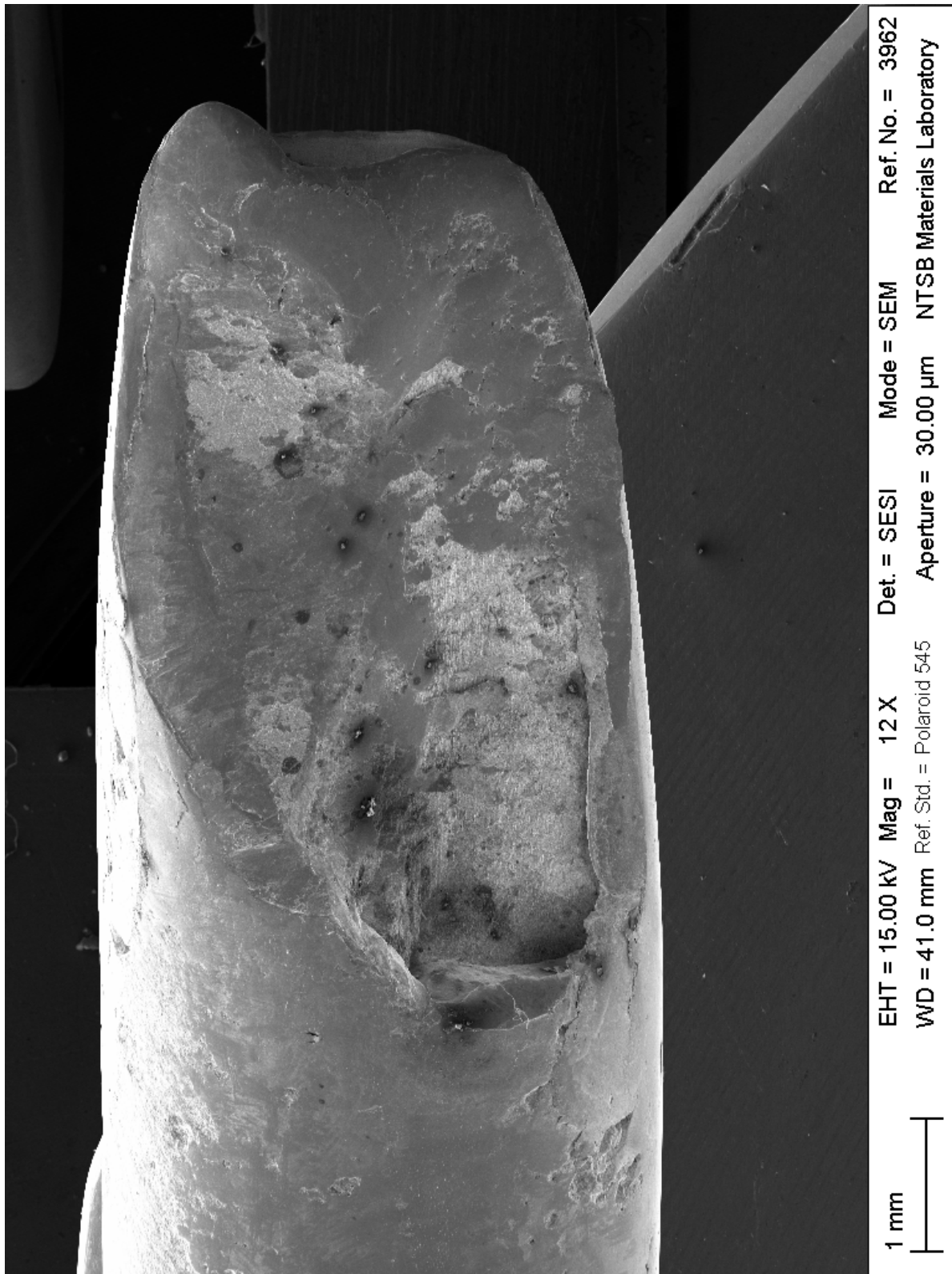


Figure 2 Overall SEM fractograph of Fracture 1A. Smooth areas indicate mechanical contact damage.

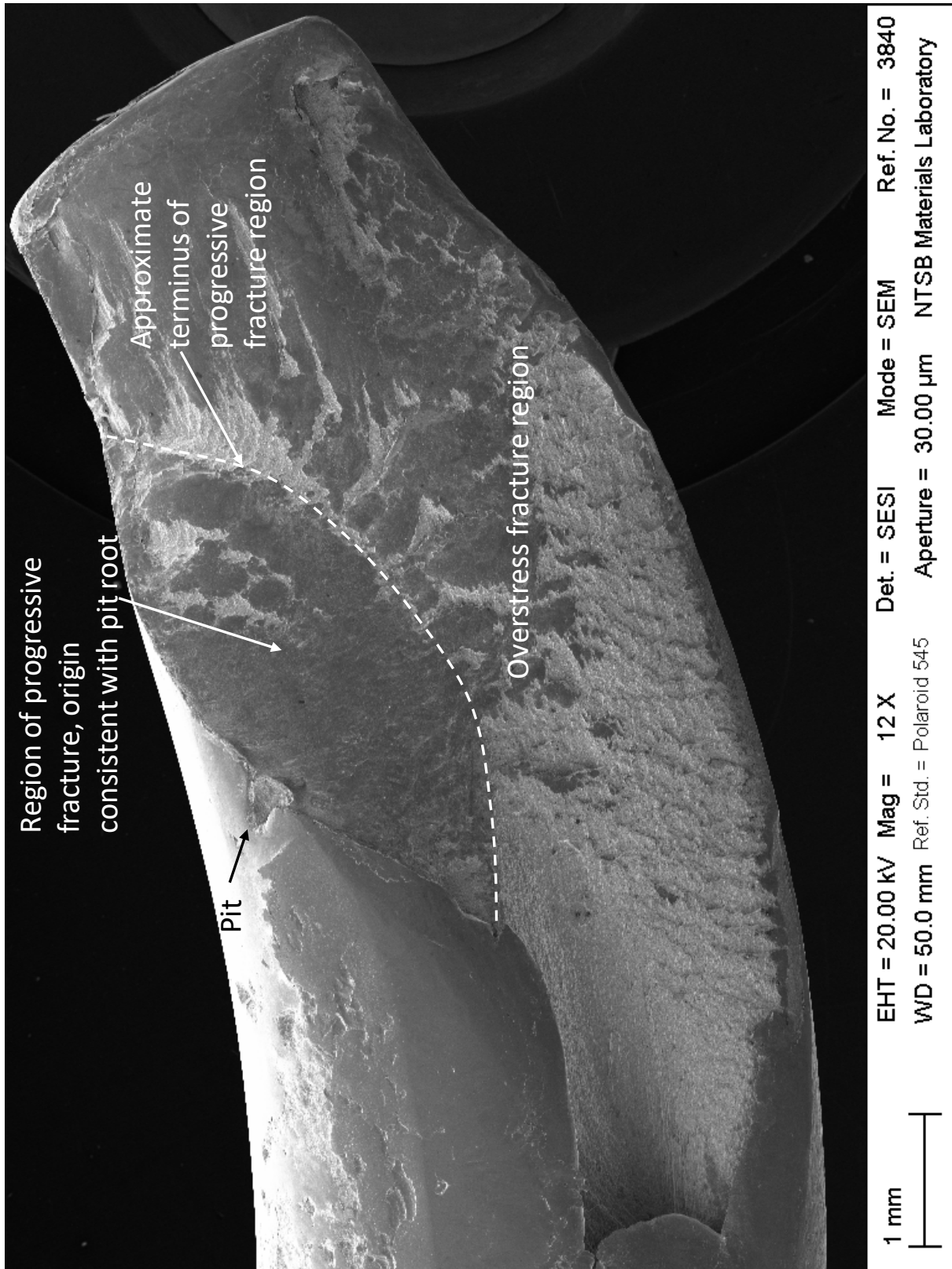


Figure 3 Overall SEM fractograph of Fracture 1B. Smooth areas indicate mechanical contact damage. Key fracture features are annotated on the image.

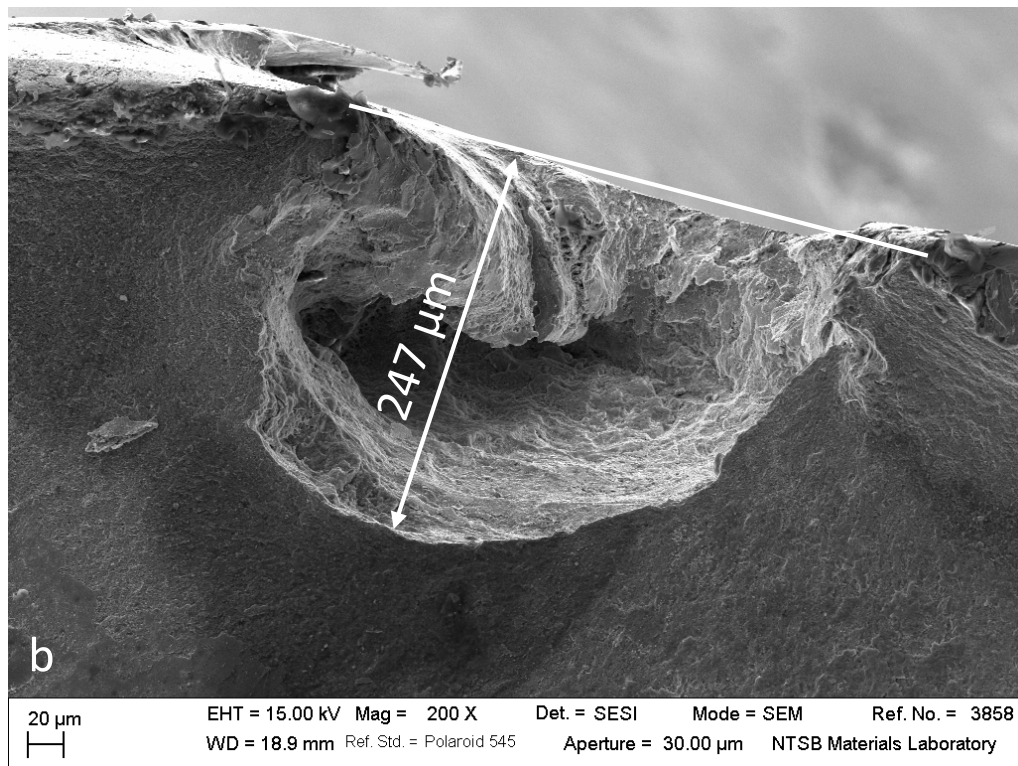
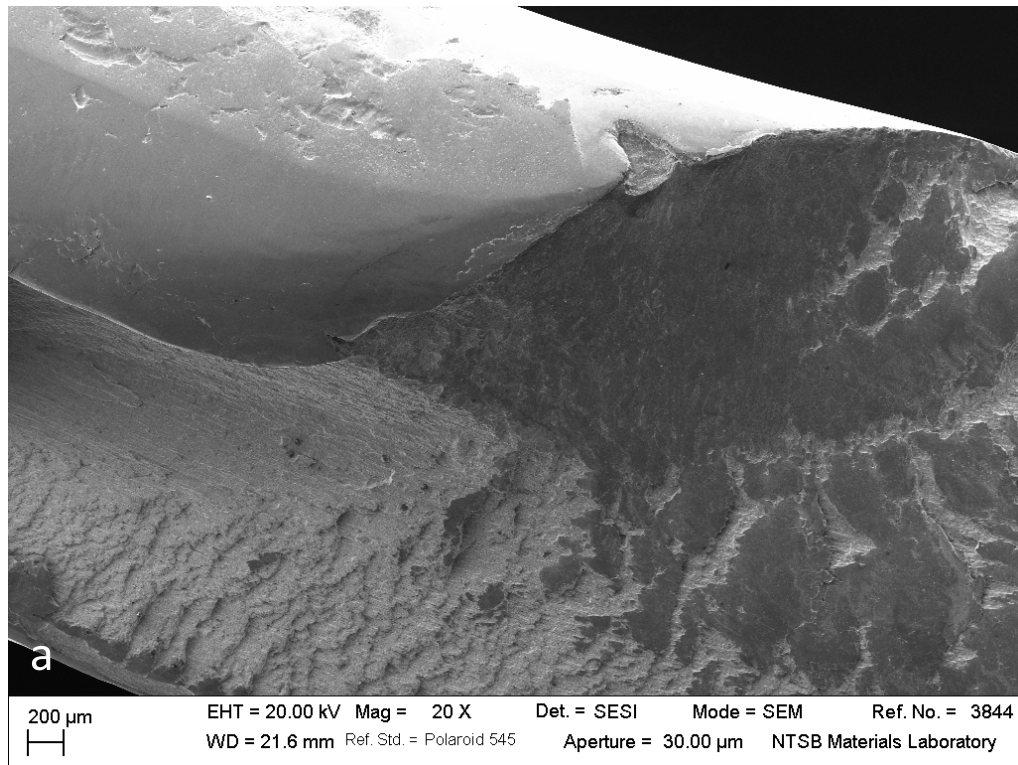


Figure 4 SEM fractographs of Fracture 1B showing closer views of the fatigue fracture-initiating surface pit in the spring wire. The approximate depth of the is shown in view b.



Figure 5 Overall SEM fractograph of Fracture 2A. Key fracture features are annotated on the image. The fatigue fracture-initiating surface pit in the spring wire is indicated.

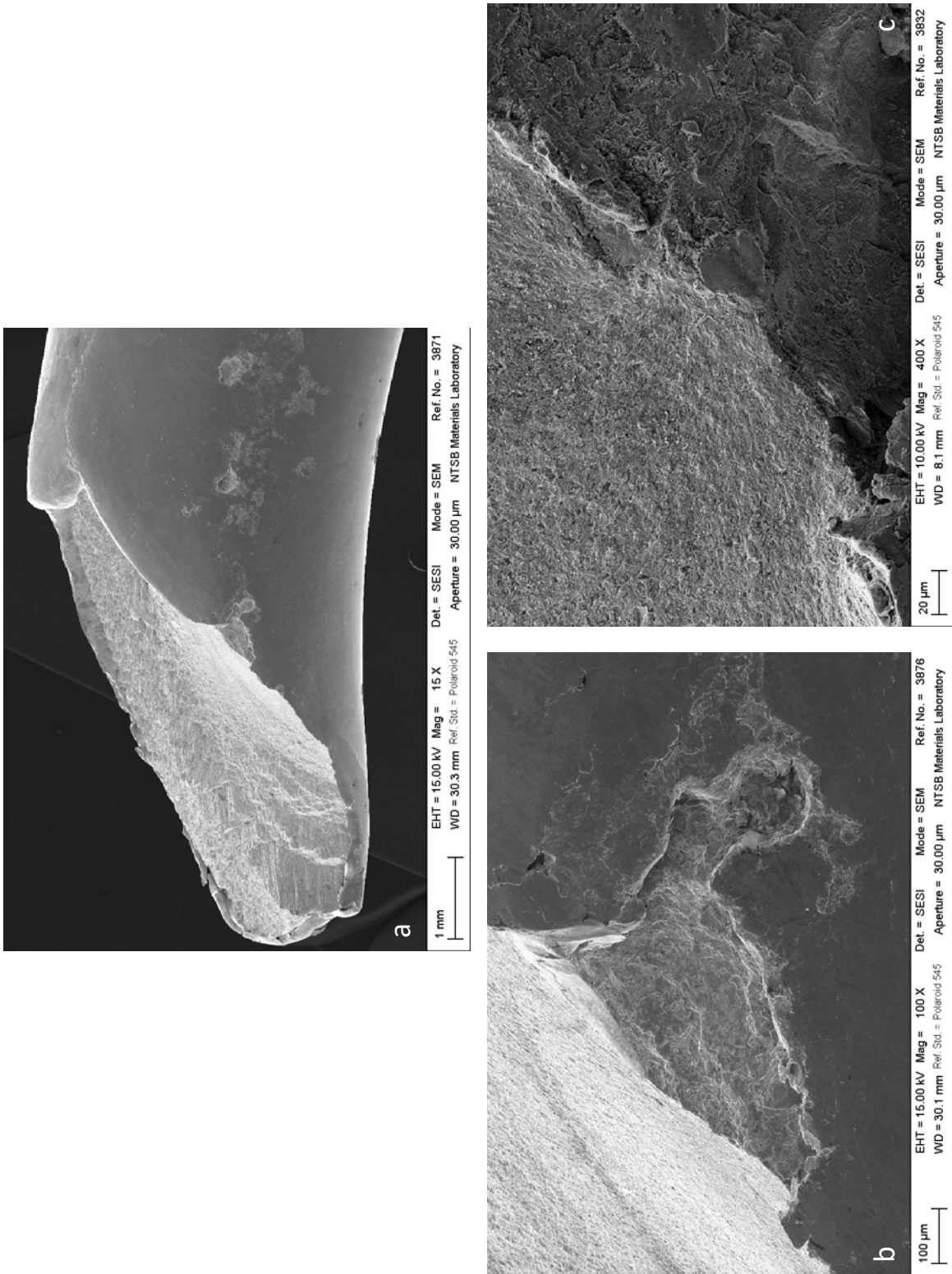


Figure 6 SEM images of Fracture 2A showing progressively higher magnification images of the fatigue fracture-initiating surface pit in the spring wire.

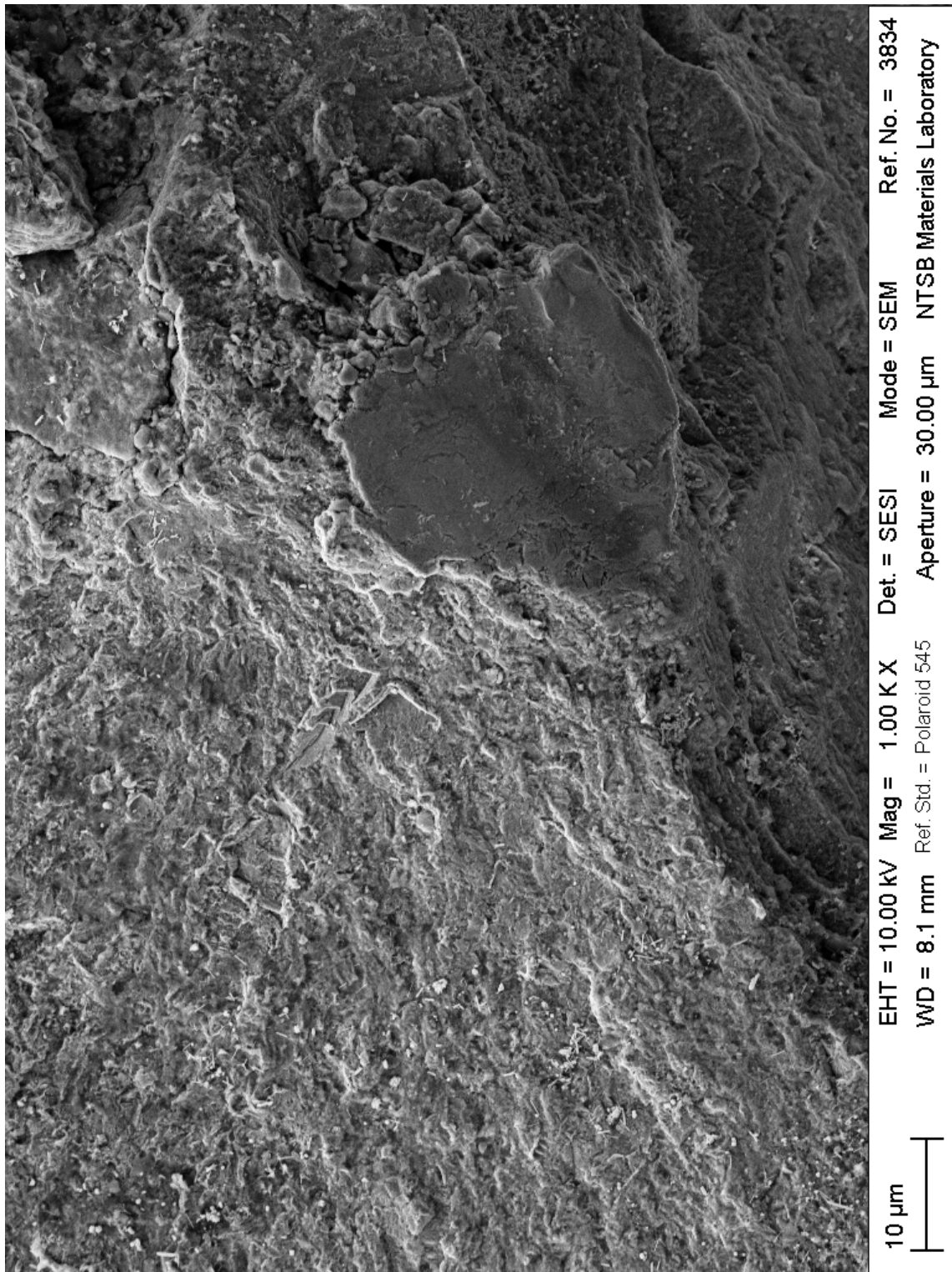


Figure 7 Higher magnification image of the fatigue crack origin area shown in Figure 6c.

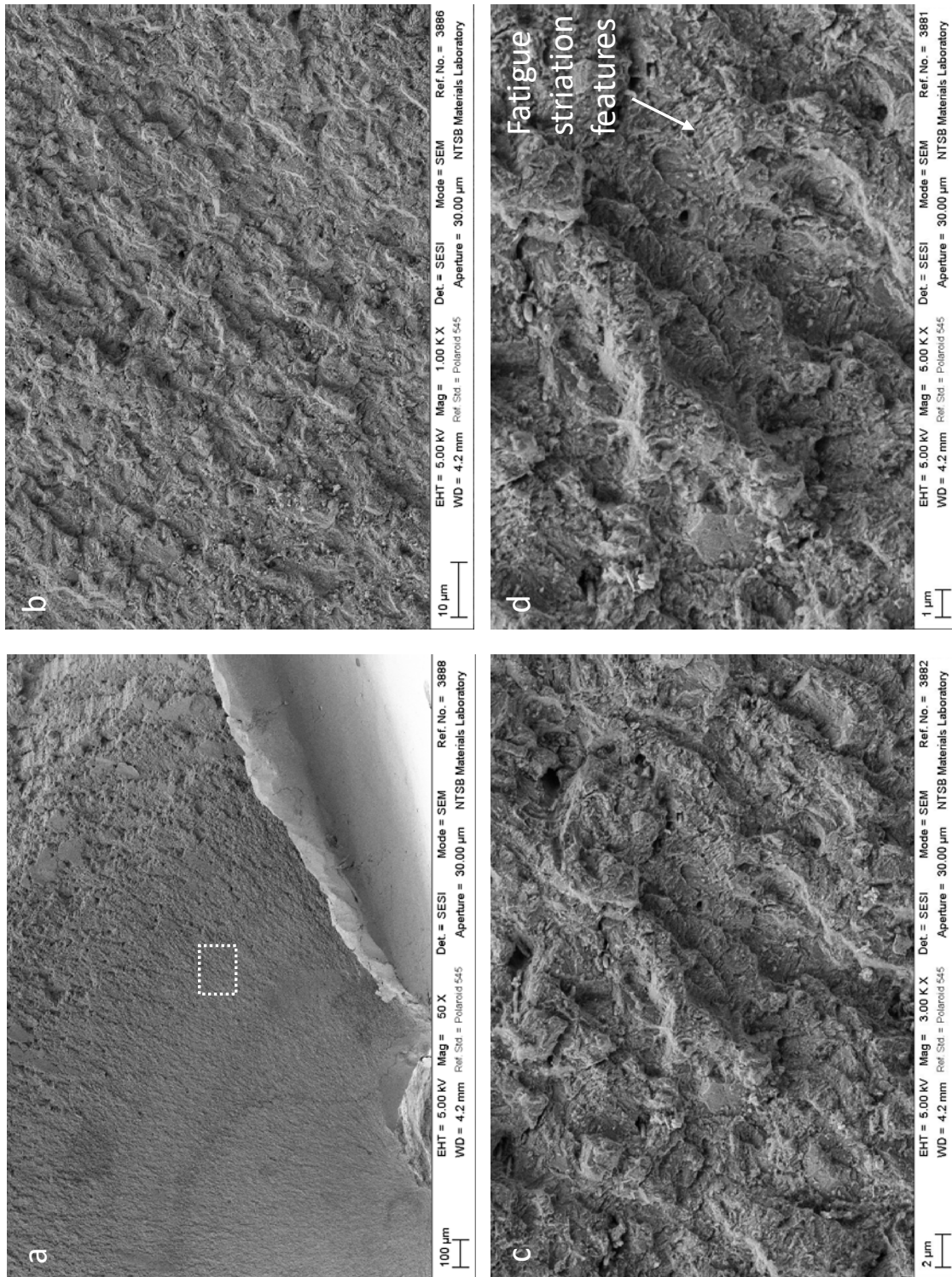


Figure 8 SEM fractographs of progressively higher magnification, showing an example fracture surface in the fatigue fracture region of Fracture 2A. Views b, c, and d are from the region marked by the dashed box in view a. Fatigue striations are noted in views c and d.

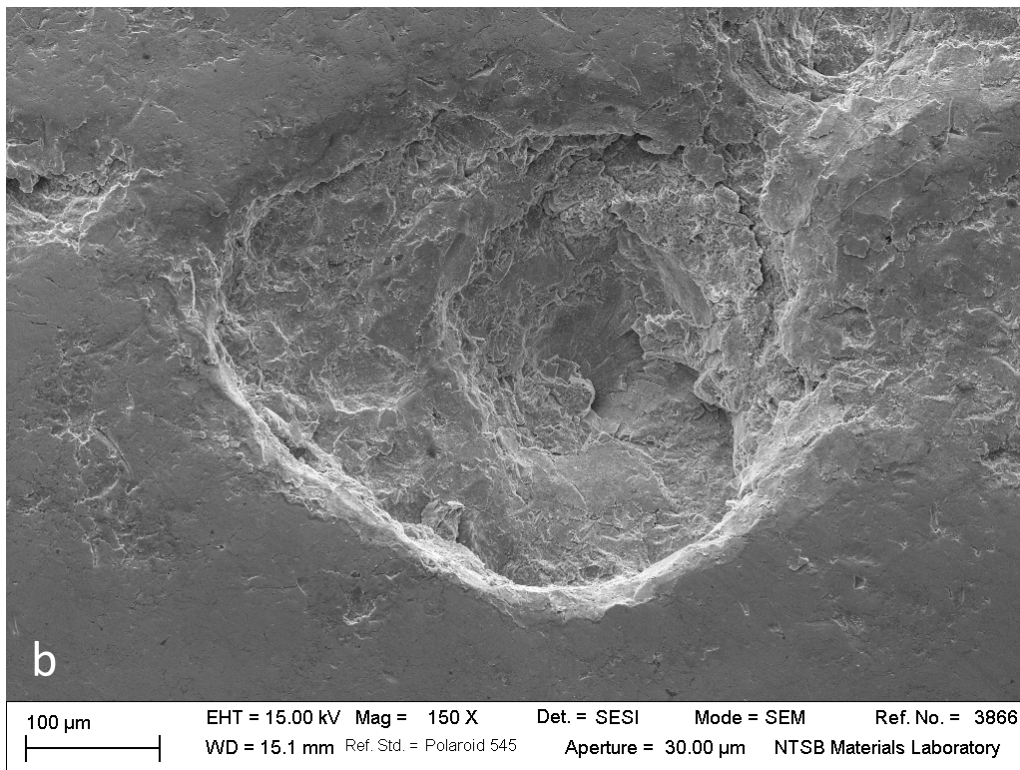
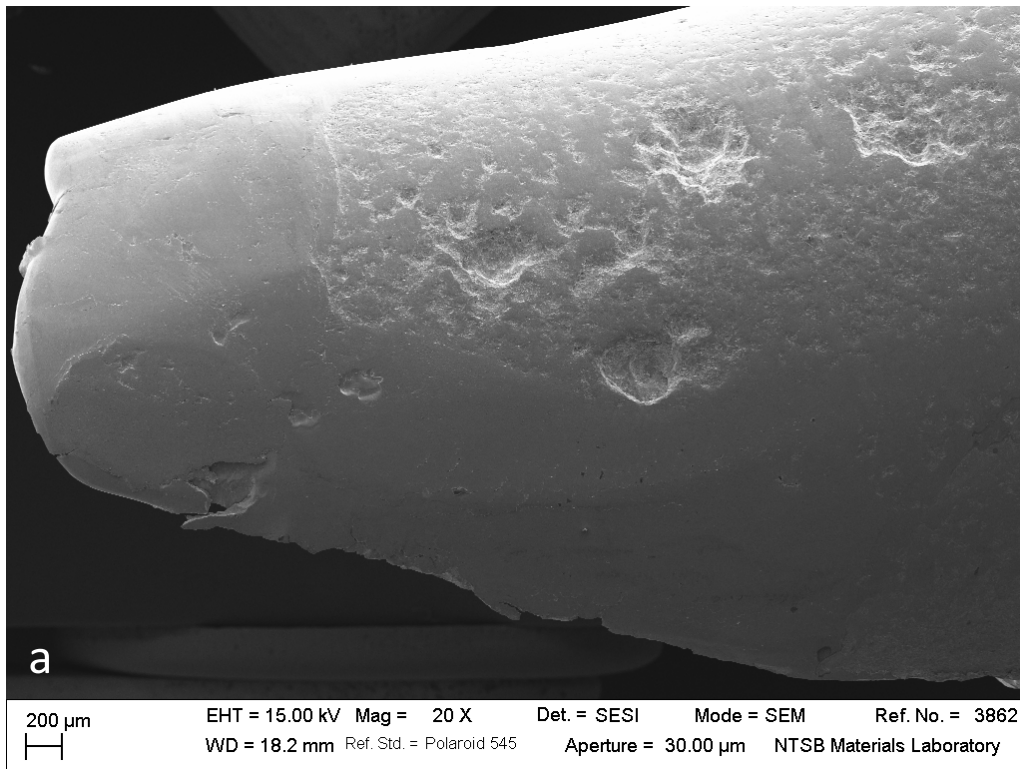


Figure 9 Close SEM images of example surface pits in the spring wire adjacent to Fracture 2A.



Figure 10 Overall SEM fractograph of Fracture 2B.



Figure 11 Overall SEM fractograph of Fracture 2B, oblique view.

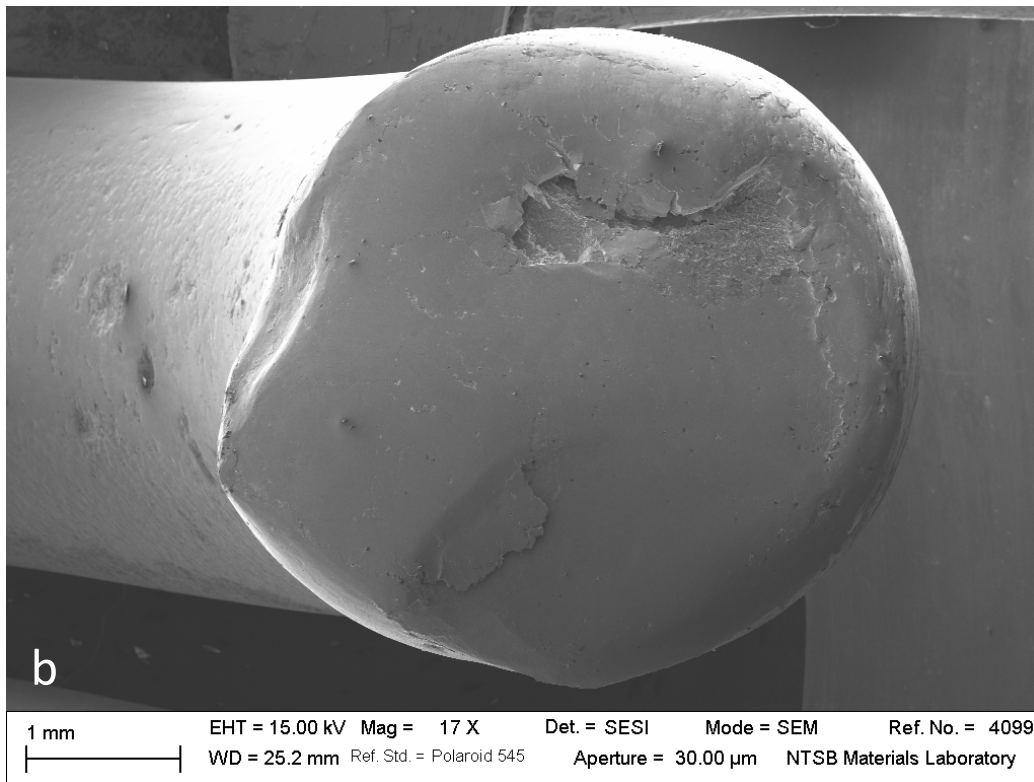
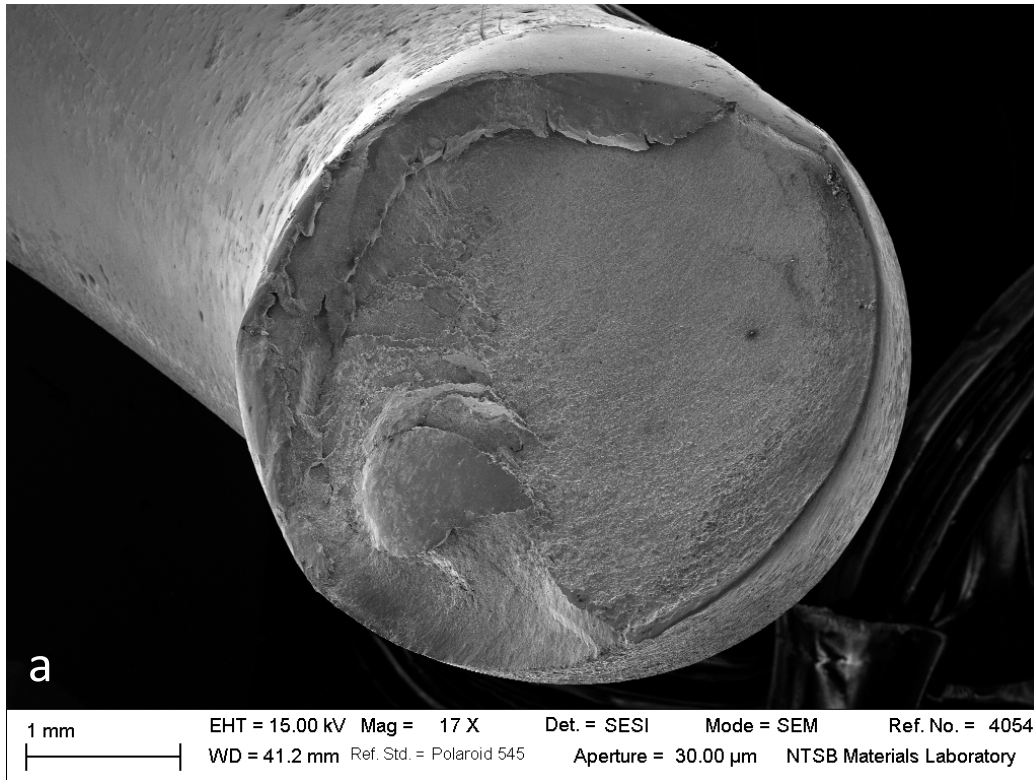


Figure 12 Overall SEM fractographs of Fracture 3. View a is Fracture 3A and view b is Fracture 3B.